Influencing the homing and differentiation of MNCs in hereditary hemorrhagic telangiectasia

Dingenouts, C.K.E.

Citation

Cover Page

Universiteit Leiden

Author: Dingenouts, C.K.E.
Title: Influencing the homing and differentiation of MNCs in hereditary hemorrhagic telangiectasia
Issue Date: 2019-02-27

4

BMP receptor inhibition enhances tissue repair in endoglin heterozygous mice

Calinda K.E. Dingenouts[1#&], Wineke Bakker[1&], Kirsten Lodder[1], Karien C. Wiesmeijer[1], Asja T. Moerkamp[1], Hans-Jurgen J. Mager[2], Repke J. Snijder[2], Cornelius J.J. Westermann[2], Margreet R. de Vries[3], Paul H.A. Quax[3], Marie-José Goumans*[1]

1. Department of Cell and Chemical Biology, Leiden University Medical Center, Leiden, The Netherlands
2. St. Antonius Hospital, Nieuwegein, the Netherlands,
3. Department of Surgery, Leiden University Medical Center, Leiden, The Netherlands

Current Address: Department of Infectious Diseases, Leiden University Medical Center, Leiden, The Netherlands

&/* Authors contributed equally

Abstract

Hereditary hemorrhagic telangiectasia type 1 (HHT1) is a severe vascular disorder caused by mutations in the TGFβ/BMP co-receptor endoglin. Endoglin haploinsufficiency results in impaired neovascularization and tissue repair after ischemic injury like myocardial infarction (MI) or hind limb ischemia. Furthermore, HHT1 patients display an impaired immune response, demonstrated by increased infection rates. To date it is still not understood to what extend immune cells are affected by the HHT1 pathology. Therefore we investigated the immune response during wound repair in Eng$^{+/-}$ mice, a model for HHT1. We observed that these mice had a prolonged period of monocyte-derived macrophage infiltration after experimentally induced MI. Moreover, there was an increased number of inflammatory Ly6C^{high}/CD206$^-$-macrophages (M1-like) at the expense of reparative Ly6C^{low}/CD206$^+$-macrophages (M2-like). Interestingly, HHT1 patients showed increased numbers of inflammatory macrophages. In vitro analysis revealed that TGFβ-induced differentiation of Eng$^{+/-}$ monocytes into M2 macrophages was blunted. Inhibiting BMP signaling by treating monocytes with BMP receptor inhibitor LDN-193189 normalized their differentiation. Systemic LDN treatment after MI improved heart function and enhanced vascularization in both wild type and Eng$^{+/-}$ mice. The beneficial effects of LDN were also observed in the hind limb ischemia model. While blood flow recovery was hampered in vehicle treated animals, LDN treatment improved tissue perfusion recovery in Eng$^{+/-}$ mice. In conclusion, BMPR inhibition restores HHT1 macrophage imbalance in vitro and improves tissue repair after ischemic injury in Eng$^{+/-}$ mice.

4

Introduction

Endoglin (also known as CD105) is a transmembrane protein that functions as a co-receptor for Transforming Growth Factor-β (TGFβ)1 and TGFβ3. Mutations in endoglin resulting in haploinsufficiency are the cause of the autosomal dominant vascular disorder *Hereditary Hemorrhagic Telangiectasia type 1 (*HHT1). HHT1 is rare life-threatening disorder characterized by local angiodysplasia like arterial venous malformations, telangiectasia and recurrent epistaxis. Besides vascular dysplasia, an impaired immune response was also observed in HHT1 patients, evident by e.g. increased infection rates in the brain, joints and liver[1]. To gain more insight into the etiology of HHT1, the murine model for HHT1, the endoglin heterozygous (*Eng*^{+/-}) mouse, has been extensively studied. Similar to HHT1 patients, *Eng*^{+/-} mice display decreased wound healing[2] and impaired resolution of inflammation[3]. We have previously shown that *Eng*^{+/-} mice also have a delay in blood flow recovery and a reduction of collateral artery and capillary formation after hind limb ischemia (HLI)[4]. Furthermore, *Eng*^{+/-} have reduced myocardial repair after experimentally induced myocardial infarction (MI)[5], and systemic application of wild type mononuclear cells (MNCs) stimulated revascularization of the injured myocardium and restored cardiac recovery of *Eng*^{+/-} mice, an effect not seen when MNCs of HHT1 patients were used[5]. The exact role of endoglin in inflammation and tissue repair is not yet completely understood, but a rapid increase in expression levels of endoglin during the inflammatory phase of wound healing suggests endoglin is involved in these processes[6-8]. Furthermore, while in healthy individuals the expression of endoglin is upregulated in activated monocytes[9], this response is impaired both in HHT1 patients[10] and *Eng*^{+/-} mice[11], resulting in e.g. an increased infection rate and leukopenia[1,3,11,12].

Endoglin exerts its effect by modulating TGFβ and bone morphogenetic protein (BMP) signaling, two pathways proven to be essential during cardiovascular development and disease[13,14], inflammation and tissue repair[15-20]. TGFβ is the prototypic member of a large family of growth factors to which also the activins and BMPs belong[13]. Upon tissue damage, TGFβ is released from the extracellular matrix, and/or secreted by activated fibroblasts, endothelial cells, platelets, macrophages and T-cells[21-23]. TGFβ signaling is initiated by binding of the ligand to a complex of type I and type II (TβRII) transmembrane receptors. In endothelial cells and macrophages, TGFβ can propagate the signal by forming a complex between the TβRII and a type I receptor known as activin receptor-like kinase (ALK). Signaling via the type I receptor ALK5 results in phosphorylation of the transcription factors Small mothers against decapentaplegic (Smad)2 and Smad3. Complex formation of TβRII and the type I receptor ALK1 is followed by activation of Smad1 and Smad5. ALK1 can only signal via TGFβ by forming a heterotetrameric complex consisting of two TGFβ type II receptors, ALK1 and ALK5, in the presence of endoglin as co-receptor[24-26]. In the absence of endoglin, major vascular defects and impaired angiogenesis are observed, which can only partly be explained by malfunctioning of the endothelial cells by enhanced TGFβ/ALK5 signaling. It is however not known what the role of endoglin deficiency in monocytes entails and how this contributes to vascular repair after an ischemic event.

Cardiac repair after MI can be divided in 3 phases: the ischemic phase, the inflammatory phase and the regenerative phase[27]. During the ischemic phase, cells within the obstructed area are devoid of oxygen and nutrients and go into apoptosis or necrosis. In the inflammatory phase, cellular debris within the injured myocardium are resolved by recruitment of immune cells, inflammatory-like macrophages (M1-like, from here onwards referred to as 'M1'), secretion of cytokines and degradation of extracellular matrix[27]. Approximately 5 days post-MI, the regenerative phase starts and is hallmarked by the

release of cytokines stimulating vascularization, recruitment of endothelial progenitor cells and differentiation of regenerative-like macrophages (M2-like, from here onwards referred to as 'M2')[27,28]. The immune cells resolve after 2-3 weeks and a fibrous scar is formed[27]. Although we have shown impaired vascular recovery after ischemic injury in *Eng*^{+/-} mice using two different models[4,5,29], as well as a disbalance in M1/M2 macrophages[29], the relation between these two observations and endoglin heterozygosity is still poorly understood. Therefore, the aim of this study is to elucidate the effect of endoglin heterozygosity on M1 and M2 macrophages during the different phases of cardiac recovery. We show that hampered differentiation of *Eng*^{+/-} monocytes into M2 macrophages contributed to the impaired tissue repair. Moreover, the impaired macrophage differentiation was confirmed in monocytes of HHT1 patients, which could be restored by inhibiting BMP signaling. Finally, BMP receptor inhibition improved tissue repair of both the *Eng*^{+/-} ischemic myocardium as well as the *Eng*^{+/-} ischemic hind limb.

Methods

Clinical studies
The procedures performed were approved by the medical ethics committee of the St. Antonius Hospital Nieuwegein, the Netherlands. The study conforms to the principles outlined in the 1964 Declaration of Helsinki and its later amendments. All persons gave their informed consent prior to their inclusion in this study. Venous blood samples from 7 HHT1 patients and 5 age- and gender-matched healthy human volunteers were collected. Peripheral blood MNCs were isolated by density gradient centrifugation using Ficoll Paque Plus (GE Life sciences, #17-1440-02), according to the manufacturer's protocol.

Animals
All mouse experiments were approved by the regulatory authorities of Leiden University (the Netherlands) and were in compliance with the guidelines from Directive 2010/63/EU of the European Parliament on the protection of animals used for scientific purposes. Experiments were conducted in 10-12 weeks old *Eng*^{+/+} and *Eng*^{+/-} male or female C57BL/6Jico mice (Charles River).

Myocardial infarction
Myocardial infarction (MI) was induced in male mice, as described before [35]. Briefly, mice were anesthetized with isoflurane (1.5-2.5%), intubated and ventilated, after which the left anterior descending coronary artery was permanently ligated. The mice were given the analgesic drug Temgesic, both pre-operative and 24hrs post-operative to relieve pain. Mice were randomly allocated to the treatment or placebo control groups. Placebo or LDN-193189 (2.0 mg/kg, Axon Medchem, #Axon1509) was administered twice daily via intraperitoneal injection from 2 days after MI till day 14. Heart function was measured by echocardiography 14 days post-MI after which the hearts were isolated and fixated in 4% paraformaldehyde (in PBS) and embedded in paraffin.

Animal health and behavior were monitored on a daily basis by the research and/or animal care staff, all trained in animal care and handling. Humane endpoints were observed as the following criteria and symptoms: when mice displayed reduced mobility, decreased grooming, and/or impaired reaction to external stimuli. In addition, for 3 days post-MI and onwards: when the incision area displayed bleeding, swelling, redness and/or discharge, the mice would be euthanized by carbon dioxide. The mice were weighed at the day of surgery and at the echocardiography time points and euthanized when more than 15% loss of weight occurred. Mice that died before meeting the criteria for euthanasia –just after myocardial infarction or within 10 days post-MI- died because of cardiac rupture due to the deterioration of cardiac tissue.

Cardiac function measurements
Mice were anesthesized with isoflurane (1.5-2.5%), after which echocardiography was performed and recorded using the Vevo 770 (VisualSonics, Inc., Toronto, CA) system, using a 30 MHz transducer (RMV707B). Imaging was performed on the longitudinal axis of the left ventricle using the EKV (Electrocardiography-based Kilohertz Visualization) imaging mode. The percentage ejection fraction was determined by tracing of the volume of the left ventricle during the systolic and diastolic phase using the imaging software Vevo770 V3.0 (VisualSonics, Inc., Toronto, CA).

Hind limb ischemia and perfusion imaging
Hind limb ischemia (HLI) was induced as described before[30]. In brief, male and female mice were anesthetized by intraperitoneal injection of midazolam (8.0 mg/kg, Roche Diagnostics), medetomidine (0.4 mg/kg, Orion), and fentanyl (0.08 mg/kg, Janssen Pharmaceuticals). Ischemia of the left hind limb was induced by electrocoagulation of the left femoral artery, the right hindlimb served as control. After surgery, anesthesia was antagonized with flumazenil (0.7 mg/kg, Fresenius Kabi), atipamezole (3.3 mg/kg, Orion), and buprenorphine (0.2 mg/kg, MSD Animal Health). Blood flow recovery to the hind limb was measured using laser Doppler perfusion imaging (LDPI, Moore Instruments). During LDPI measurements, mice were anesthetized by intraperitoneal injection of midazolam (8.0 mg/kg, Roche Diagnostics) and medetomidine (0.4 mg/kg, Orion). After LDPI, anesthesia was antagonized by subcutaneous injection of flumazenil (0.7 mg/kg, Fresenius Kabi) and atipamezole (3.3 mg/kg, Orion). Humane endpoints after induction of HLI were observed as the following criteria and symptoms: when mice displayed reduced mobility, decreased grooming, and/or impaired reaction to external stimuli. Furthermore, when the incision wound area displayed bleeding, swelling, redness and/or discharge, the mice would be euthanized by carbon dioxide.

Immunohistochemistry
Hearts were dissected from carbon dioxide-euthanized mice, fixated overnight at 4^0C in 4% paraformaldehyde (in PBS), dehydrated and embedded in paraffin wax. Hearts were cut in 6 μm sections, mounted onto coated glass slides (VWR SuperFrost Plus), and stained for the presence of macrophages in the infarct border zone using rat anti-mouse MAC3 (CD107b, dilution 1:200, BD Biosciences, #550292) and goat anti-rat biotinylated secondary antibody (1:300, Vector Laboratories, #BA-9400). An avidin/biotin-based DAB peroxidase staining was used (Vectastain ABC system, Vector Laboratories, #PK-4000) to detect antibody

binding, next to a hematoxylin counterstain for cell nuclei.

Infarct size was determined by Picrosirius Red (PSR) collagen staining; slides were deparaffinized and hydrated, followed by 1 h incubation with PSR solution; 0.1gram Sirius Red F3B (Merck) dissolved in 100 ml saturated picric acid solution (pH=2.0) (Sigma, #P6744). Slides were washed in acidified water, dehydrated in ethanol and mounted with Entellan (Merck) mountant.

Immunofluorescent stainings were performed using standard protocol as previously described[31] for visualization of capillaries by PECAM (CD31, dilution 1:800, Santa Cruz , #sc-1506), arteries by both PECAM (CD31, dilution 1:800, Santa Cruz Biotechnology Inc.) and αSMA (alpha smooth muscle actin, dilution 1:500, Abcam) and macrophages were stained with CD11b (MAC-1, dilution 1:200, Biolegend, #1012505, clone M1/70), MAC-3 (CD107b, dilution 1:200, BD Biosciences, #550292) and CD206 (dilution 1:300, Abcam, #ab64693). Simultaneously detection of p-Smad1/5/8 (dilution 1:100, Cell signaling, #9511) was performed by 30 min antigen retrieval and subsequently p-Smad2 (dilution 1:200, Cell signaling, #3101) was amplified using a TSA™-Biotin System (Tyramide Signal Amplification) Kit (Perkin Elmer Life Science, #NEL700A). Fluorescent-labelled secondary antibodies (ThermoFisher Scientific) were incubated for 1.5 h, at 1:250 dilutions. Sections were mounted with Prolong® Gold Antifade mountant with DAPI (ThermoFisher Scientific, # P36931).

4

Isolation of immune cells from murine hearts
Hearts were harvested from the mice 4 days post- MI and put in PBS buffer on ice. After excision of the left ventricle, the tissue was put into 1ml digestion buffer (450U Collagenase A, Sigma Aldrich, # 10103578001, 60U hyaluronidase, Sigma Aldrich, #H3506, 60U DNAse-1, Roche, #10104159001) at 37°C for 1 h. The tissue homogenate was filtered through an 80µm cell strainer (Falcon # 352350) and MNCs were isolated using Ficoll density gradient specific for small mammalians (Histopaque-1083, Sigma Aldrich # 10831). Flow cytometry and staining was performed as described below.

Flow cytometry
Mouse monocytes from either 50 µL of whole blood, bone marrow mononuclear cells, or from heart lysates were stained for CD11b (with anti-mouse CD11b, BD Biosciences, #561114), Ly6C (Bio-rad Laboratories, # MCA2389A647T or BD Biosciences, #561085) and CD206 (Bio-rad Laboratories, #MCA2235A488T), to identify M1 and M2 macrophages respectively.

Human monocytes were isolated from peripheral blood, by ficoll gradient separation. Total MNCs ($3×10^5$ cells per sample) were stained with anti-CD14-ECD (Beckman Coulter, IM2707U) and anti-CD16-APC (Beckman Coulter, # A66330). Fluorescence was measured with LSRII flow cytometer (BD Biosciences) and analyzed by FACS Diva (BD Biosciences) and FlowJo software (FlowJo LLC).

Cultured macrophages from mouse bone marrow
Monocytes were isolated from the bone marrow using CD11b+ magnetic beads (Miltenyi

Biotec MACS #130-049-601) and subsequently cultured in RPMI medium (Gibco RPMI 1640 Medium, #11875-093), supplemented with 10% FBS (Fetal Bovine Serum, Gibco, ThermoFisher Scientific, #10270) and 1ng/ml GM-CSF (Peprotech, #315-03) to induce differentiation into macrophages. After 3 days, the attached cells were stimulated with TGFβ3 (1 ng/ml, kind gift of Dr. K. Iwata), ALK5 kinase was inhibited using SB-431542 (10μM, Tocris, #1614), BMPR type I (ALK1/2/3) were inhibited using LDN-193189 (100nM, Axon Medchem, #Axon1509) addition for 4 days.

Western blot analysis

For intracellular protein analysis, at day 6 of culture the macrophages were serum starved overnight after which they were either stimulated or not for 1 h with TGFβ and/or inhibitors at the indicated concentrations, after which cells were lysed with RIPA lysis buffer (5 M NaCl, 0.5 M EDTA, pH 8.0, 1 M Tris, pH 8.0, NP-40 (IGEPAL CA-630), 10% sodium deoxycholate, 10% SDS, in dH_2O) supplemented with phosphatase inhibitors (1M NaF Sigma Aldrich # S7920, 10% NaPi Avantor #3850-01, 0.1M NaVan Sigma Aldrich # S6508) and protease inhibitors (Complete protease inhibitor cocktail tablets, Roche Diagnostics, #11697498001). Protein concentration was measured using Pierce BCA protein assay (ThermoFisher Scientific, #23225). Equal amounts of protein were loaded onto 10% SDS-polyacrylamide gel and transferred to an Immobilon-P transfer membrane (PVDF membrane, Millipore, # IPVH00010). The blots were blocked for 1 h using 5% milk in TBST (Tris-buffered saline, 0.1% Tween20) solution and incubated O/N with rabbit anti-mouse phosphorylated Smad2 (Cell signaling, #3101), total Smad2/3 (BD Biosciences, BD610842), mouse anti-mouse phosphorylated ERK1/2 (Sigma-Aldrich, #M8159), rabbit anti-mouse total ERK1/2 (p44/42 MAPK, Cell Signaling, #4695, clone 137F5), rabbit anti-mouse phosphorylated p38 (Cell Signaling Technology, #9211) and mouse anti-rabbit total p38 (Santa Cruz Biotechnology Inc. #535). Blots were incubated for 60 minutes with horse radish peroxidase anti-rabbit (ECL rabbit IgG, HRP-linked whole Ab, GE Healthcare, #NA934V) or anti-mouse (ECL mouse IgG, HRP-linked whole Ab, GE Healthcare, #NA931V) antibodies. Blots were developed in an X-omat 1000 processor (Kodak) with SuperSignal West Dura Extended Duration Substrate (ThermoFisher Scientific, #37071) or SuperSignal West Pico Chemiluminescent Substrate (ThermoFisher Scientific, # 34080AB) and exposed to SuperRX medical X-ray film (Fujifilm Corporation). Analysis was performed using Image J (Version 1.51, National Institutes of Health, USA). Full-length blots are included in the Supplementary Information file.

Statistical analysis

Statistical significance was evaluated by unpaired Student's t-test between 2 groups or ANOVA with Bonferroni correction to test between multiple groups with GraphPad Prism 6 software. Values are represented as meanSD or SEM when otherwise indicated. Values of $P<0.05$ are denoted as statistically significant.

Data availability

No datasets were generated or analyzed during the current study. The results generated during and/or analyzed during the current study are available from the corresponding author on reasonable request.

Results

Endoglin deficiency results in prolonged inflammation and reduced M2 macrophage presence after MI

Recruitment of inflammatory cells and timely resolution is essential for cardiac tissue repair. An inadequate or excessive inflammatory response is detrimental in the injured myocardium and can lead to adverse remodeling. We therefore investigated the effects of endoglin heterozygosity on the influx of monocytes during the inflammation phase after experimentally induced MI. We first determined if endoglin heterozygosity influences MNC composition at baseline. Before induction of MI, we observed no differences in MNC subtypes, like macrophages, lymphocytes, NK-cells, neutrophils and granulocytes in blood and bone marrow between wild type (WT, $Eng^{+/+}$) and endoglin heterozygous ($Eng^{+/-}$) mice (data not shown). Subsequently we induced MI and assessed the number of macrophages present in the heart using immunohistochemical analysis. Four days post-MI, MAC-3 expressing macrophages were present in large numbers in the border zone of the infarcted hearts of both WT and $Eng^{+/-}$ mice (Fig. 1a and b). Macrophage infiltration in the WT hearts was cleared 14 days post MI (Fig. 1a and b), confirming previous studies reporting that the inflammatory response is most pronounced at day 3-5 and cleared after approximately two weeks[27]. Interestingly, at 14 days post-MI MAC-3 expressing cells were still easily detectable in the infarct border zone of $Eng^{+/-}$ mice (Fig. 1b), suggesting a delay in macrophage resolution.

To further characterize the phenotype of these macrophages, we determined the expression of CD11b, a general monocyte/macrophage marker, and CD206, a specific marker for M2 (regenerative) macrophages facilitating the healing process. Immunofluorescent analysis of the spleen, used as control tissue, showed the presence of CD11b positive resident monocytes, while no CD206 staining was observed (Fig. 1c). Four days post-MI, hearts of WT mice harbor similar numbers of CD11b and CD206 expressing cells, suggesting that the macrophages present in the heart are M2 macrophages. In contrast, in the hearts of $Eng^{+/-}$ mice CD11b$^+$ cells were easily detectable, while only limited expression of CD206 was present. We quantified these observations using flow cytometry on single cell suspensions of mouse hearts (Fig. 1d). At day 4 post-MI the $Eng^{+/-}$ hearts contained significantly less M2 macrophages while the number of pro-inflammatory M1 macrophages was significantly increased (Fig. 1d, p<0.0001 and p=0.0011 respectively). This suggests a macrophage polarization in the injured $Eng^{+/-}$ heart towards a less regenerative macrophage phenotype.

Endoglin deficiency reduces in vitro differentiation of regenerative macrophages in both HHT1 mice and patients

To gain more insight in how endoglin heterozygosity may influence macrophage differentiation we isolated bone marrow derived CD11b+ monocytes and used immunofluorescence to analyze their differentiation towards macrophages in vitro. Endoglin is expressed on murine macrophages and co-staining of endoglin together with the inflammatory macrophage marker Ly6C, revealed that endoglin is specifically present on murine macrophages with a low expression level of Ly6C (Fig. 2a). Macrophages with high expression levels of Ly6C, known as the inflammatory-like (M1-like) subtype, show low expression levels of endoglin (Fig. 2a). More detailed analysis of the different macrophage subtypes in Eng+/- mice and HHT1 patients was performed using flow cytometry. Inflammatory (M1) macrophages were identified by the expression of CD11b, high levels of Ly6C and low CD206 expression for mouse macrophages, and the expression of CD14 and absence of CD16 expression for human cells (Fig. 2b). Regenerative (M2) macrophages were identified by the expression of CD11b,
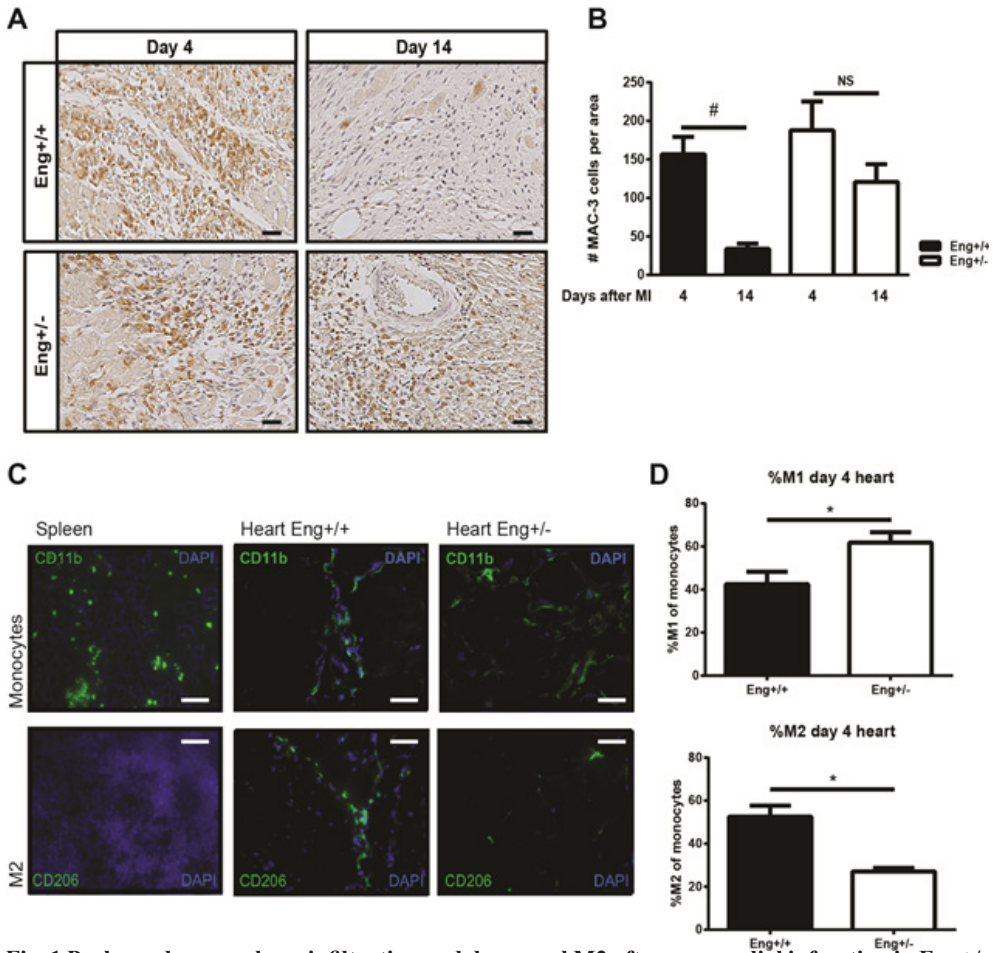
Fig. 1 Prolonged macrophage infiltration and decreased M2 after myocardial infarction in Eng+/- mice. a Cardiac sections of Eng+/+ and Eng+/- mice were stained for macrophages. Representative pictures of MAC-3 expressing macrophage (MAC-3= brown; nuclei= blue) at day 4 and 14 after MI. Scale bar: 50μm. **b** Quantification of the MAC3 positive cells at day 4 and 14 after MI in cardiac section of Eng+/+ and Eng+/- mice. N=5-16 mice per group. **c** To determine the number of M1 vs M2 monocytes splenic tissue and infarcted cardiac muscle tissue were stained with CD11b as a general monocyte marker and CD206 as M2 macrophage marker 4 days after MI. Scale bar: 50μm. **d** To quantify the two macrophage subtypes, the ratio M1/M2 macrophages was determined by flow cytometry using a single cell suspension of Eng+/+ and Eng+/- mice hearts 4 days post MI. The inflammatory M1 macrophage was identified by CD11b+/Ly6Chigh/CD206- selection and the regenerative M2 by CD11b+/Ly6Clow/CD206+ selection. N=5-16 mice per group. * p<0.05, # p<0.001

low levels of Ly6C and high expression of CD206 for mice, and the expression of both CD14 and CD16 for human cells (Fig. 2b). Monocytes isolated from Eng+/- mice as well as HHT1 patients show an increased percentage of inflammatory macrophages (p=0.006 and p=0.008) and a reduction of regenerative macrophages, compared to macrophages from WT mice and healthy volunteers (Fig. 2c, p=0.02 and p=0.008 respectively).
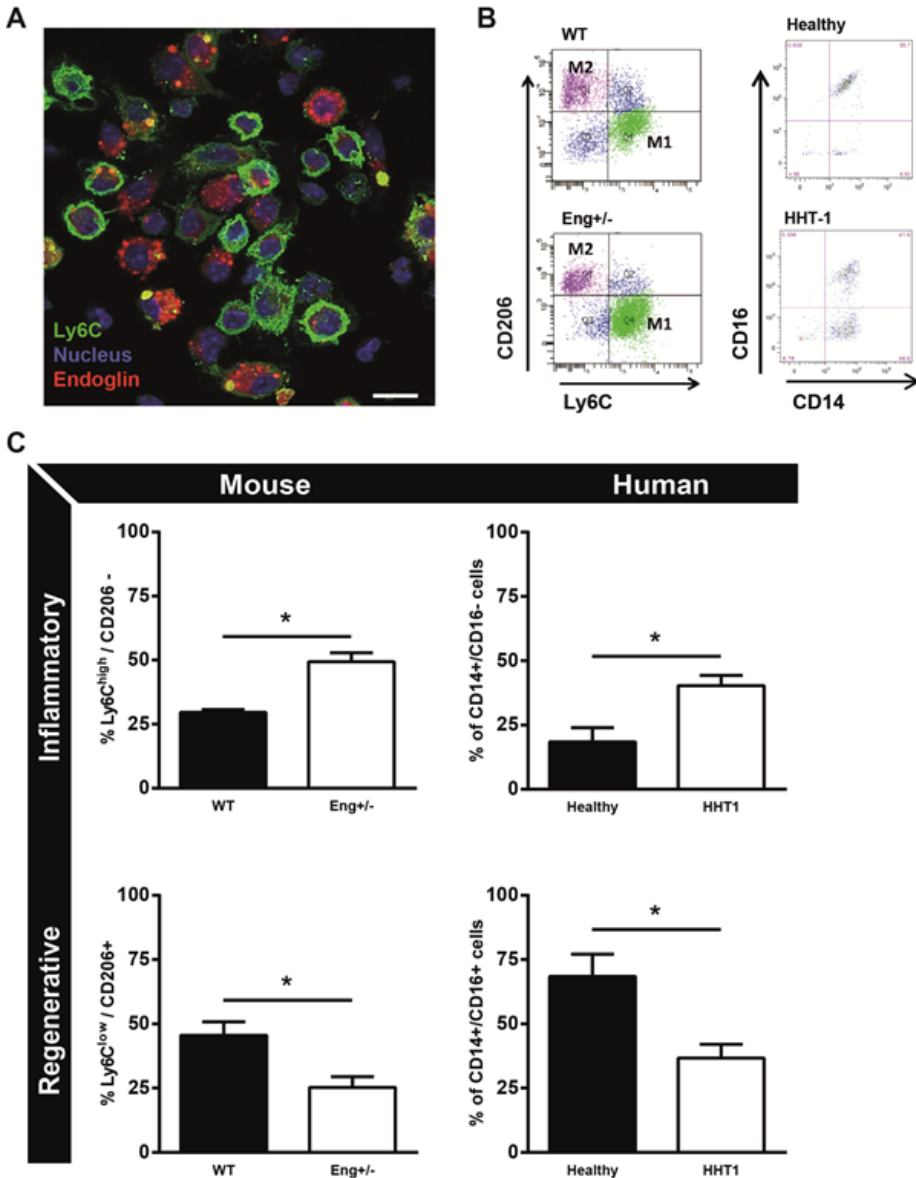
Fig. 2 Macrophage phenotype is dependent on endoglin expression.
a Macrophages isolated from WT mice were stained with endoglin (red), Ly6C (green) and dapi (nuclei, blue). Scale bar: 10μm. b Representative flow charts of mouse and human isolated monocytes of Eng+/- mice and HHT1 patients and their healthy controls. For mouse inflammatory monocytes were distinguished by CD11b+/Ly6Chigh/CD206- and regenerative monocytes by CD11b+/Ly6Clow/CD206+ expression. For human, inflammatory monocytes were distinguished by CD14+CD16- and regenerative monocytes by CD14+/CD16+ expression. c quantification of the flow cytometry data as represented in B, divided in inflammatory and regenerative monocytes of mouse and human. Mouse samples: N=5-16 mice per group. Human samples: 7 HHT1 patients and 5 age- and gender-matched healthy human volunteers. * p<0.05; **p<0.01

In vitro switch of macrophage differentiation by adaptation of the TGFβ signaling response

As endoglin is a co-receptor of TGFβ, we next investigated the effect of stimulation and inhibition of the TGFβ-signaling pathway on macrophage differentiation. Monocytes isolated from bone marrow of WT mice were cultured for 3 days in the presence of GM-CSF to stimulate their differentiation into macrophages after which 1ng/ml of TGF ligand was added for either 24 or 96 hours. While 24 hours of TGFβ stimulation had little effect on the percentage of M1 and M2 macrophages compared to non-stimulated cells, 96 hours of TGFβ stimulation skewed macrophage differentiation towards a M2 phenotype (Fig. 3a, p=0.001). This TGFβ increase in M2 macrophages was blocked by adding SB-431542 (SB), a potent ALK5 kinase inhibitor, to WT monocyte cultures, but not by adding the BMPRI inhibitor LDN-193189 (LDN) (Fig. 3b). The M1/M2 macrophage numbers did not change when monocytes isolated from *Eng*$^{+/-}$ mice were stimulated with TGFβ nor did inhibition of the ALK5 kinase by stimulating the cells with SB. Interestingly, when LDN was added to TGFβ stimulated macrophage cultures, the differentiation towards M1 macrophages was reduced, resulting in a normalization of the ratio of *Eng*$^{+/-}$ M1-M2 macrophages to WT levels (Fig. 3c).
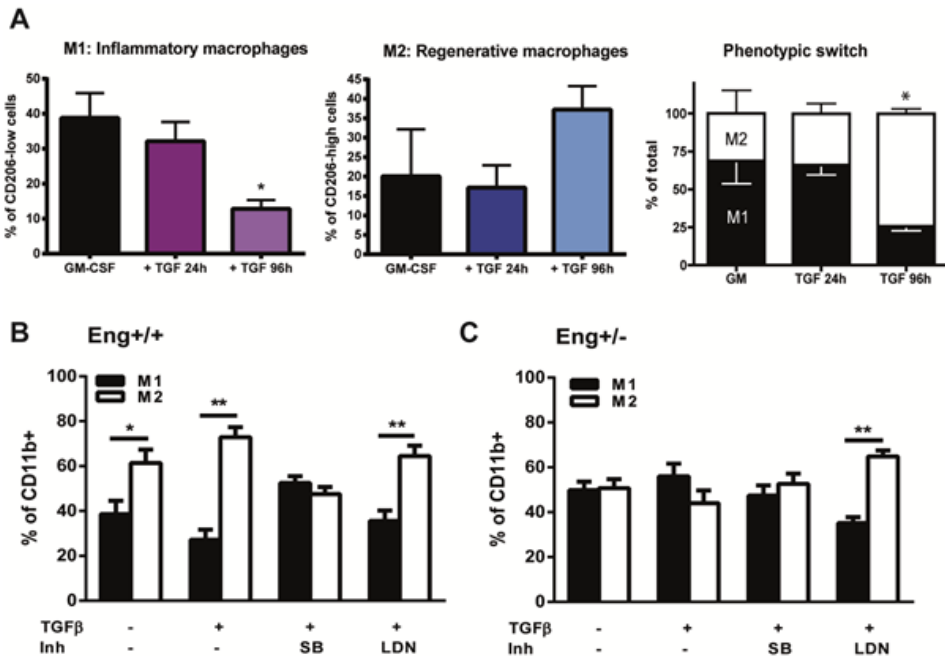

Fig. 3 TGFβ signaling influences macrophage subtype differentiation. a Macrophages from Eng+/+ mice cultured with either GM-CSF for 7 days only or in combination of TGFβ (2.5 ng/ul) for 24h and 96h. The macrophage phenotype was determined based on the expression of Ly6C high (M1) and low (M2) of the CD11b expressing macrophages. * p=0.001 difference in the number of M1 and M2 between GM-CSF vs TGFβ stimulation for 96h. b-c BM isolated monocytes from Eng+/+ (b) and Eng+/- (c) mice were cultured in the presence of GM-CSF in the presence or absence of TGFβ (2.5ng/ul), SB (10µM), or LDN (100nM). The macrophage subtype was determined based on the expression of Ly6C high (M1) and low (M2) of the CD11b expressing macrophages. *p=0.007; **p<0.0001

TGFβ/BMP and non-Smad signaling in *Eng*^{+/-} macrophages is impaired

TGFβ transduces its signal from the membrane to the nucleus by phosphorylation of downstream effectors: canonical Smads and non-canonical signaling proteins ERK and p38. To explore which pathway was used, monocytes from WT and *Eng*^{+/-} mice were differentiated into macrophages, serum starved and stimulated for 60 min with TGFβ and/or indicated inhibitors; SB or LDN. TGFβ was not able to detectably phosphorylate Smad1/5 after serum starvation in neither WT nor *Eng*^{+/-} macrophages (data not shown). For Smad2 however, both WT and *Eng*^{+/-} macrophages showed an induction of Smad2 phosphorylation upon stimulation with TGFβ, which was blocked when SB was added, but not by LDN (Fig. 4a and b). Phosphorylation of Smad2 was not different between WT and *Eng*^{+/-} macrophages. Interestingly, while LDN did not influence TGFβ-induced p-Smad2 in WT macrophages, a significant increase was observed in the *Eng*^{+/-} macrophages (Fig. 4b).
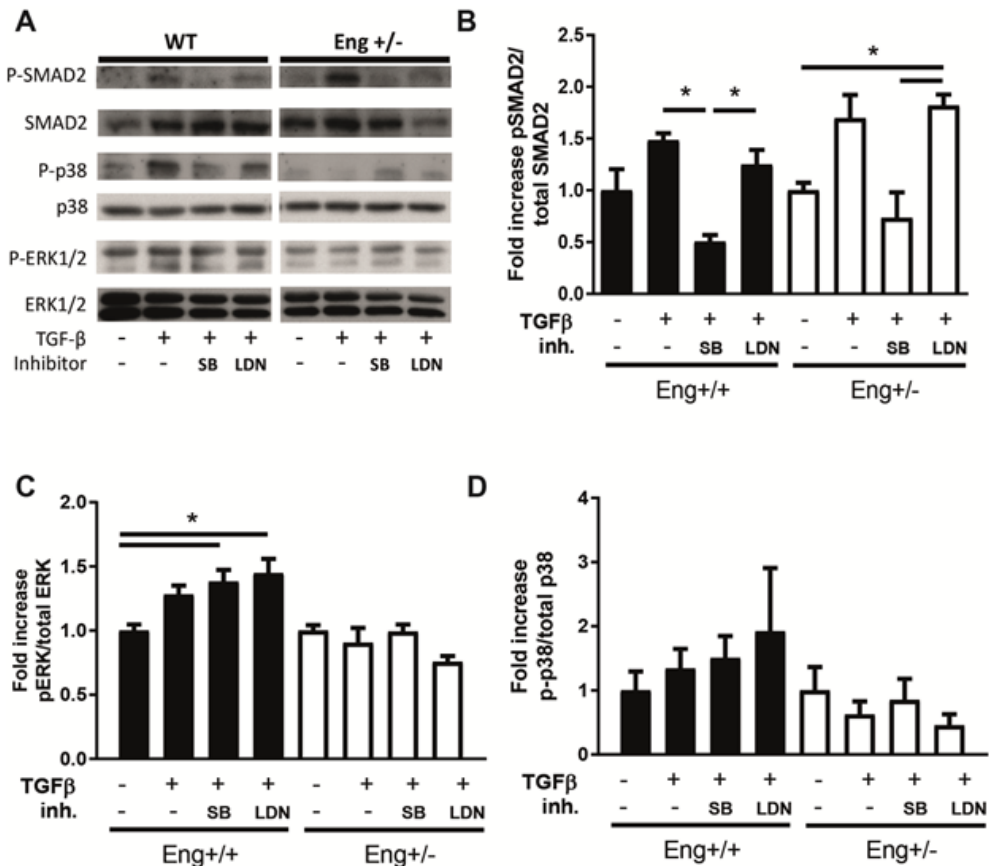

Fig. 4 Eng+/- macrophages show blunted TGFβ and BMP signaling responses in vitro. a Western blot analysis of Eng+/+ and Eng+/- cultured murine macrophages with GM-CSF, stimulated 60 min with TGFβ (2.5ng/ul), SB (10μM), LDN (100nM). Representative blots of n=3 are shown. Full-length blots are included in the Supplementary Information file. **b** Densitometric analysis of the blots shown in a has been performed, expressed as the percentage of phosphorylated Smad2 relative to total amount of Smad2 protein. N=3. **c** Quantification of the blots as shown in a, expressed as the percentage of phosphorylated ERK relative to total amount of ERK protein. N=3. **d** Quantification of the blots as shown in a, expressed as the percentage of phosphorylated p38 relative to total amount of p38 protein, N=3-4. Error bars are SEM. * p<0.05

Since TGFβ can also signal via Smad independent pathways[32-34], we next analyzed the non-canonical pathways known to be involved in stress, inflammation and differentiation responses: the MAPK and p38 pathways. ERK1/2 phosphorylation was increased in WT macrophages upon stimulation with TGFβ, and was further enhanced when SB or LDN were added to TGFβ-stimulated WT macrophages (Fig. 4a and c). Macrophages derived from *Eng*^{+/-} mice did not show an effect on ERK1/2 phosphorylation when stimulated with TGFβ, neither in the presence nor absence of SB or LDN (Fig. 4c). Phosphorylation of p38 showed the same trend as ERK; an increase in p-p38 in WT cells upon TGFβ stimulation and further enhancement in the presence of SB or LDN, while there was no response or even a trend towards reduced p-p38 in *Eng*^{+/-} macrophages (Fig. 4a and d). In summary, *Eng*^{+/-} macrophages show increased Smad2 phosphorylation when BMP signaling is inhibited, while the non-canonical pathways show decreased responsiveness.
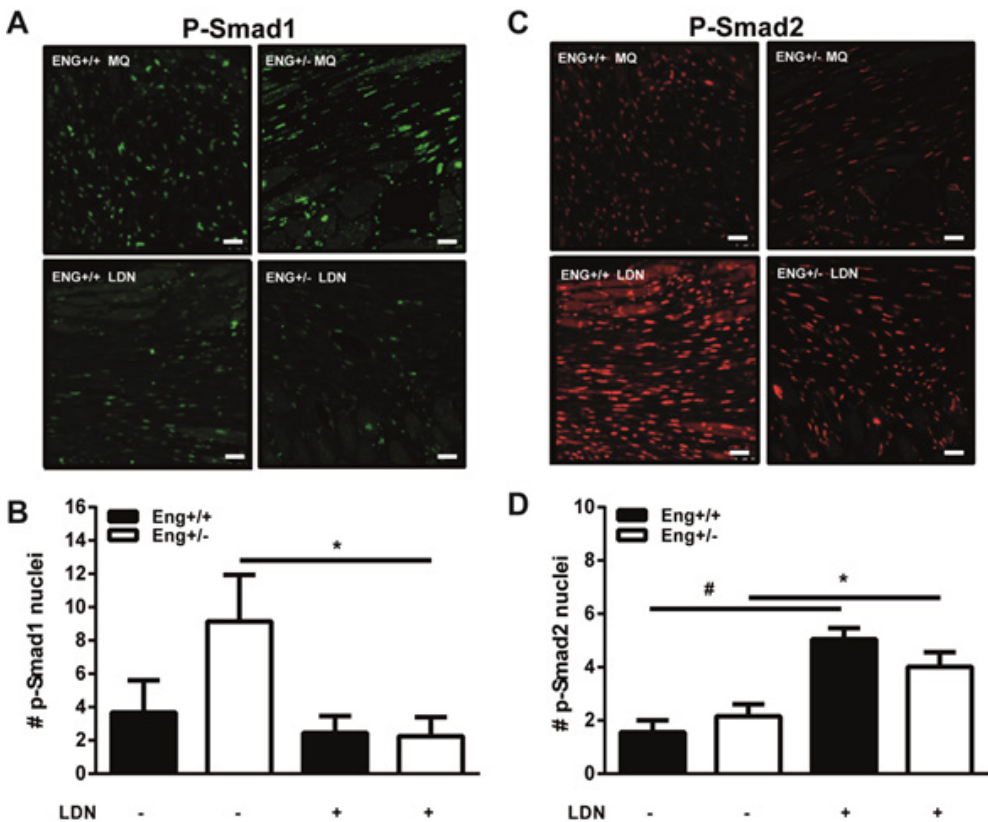

Fig. 5 LDN decreases p-Smad1 and induces p-Smad2 in the infarct border zone.
a   Paraffin heart sections were stained for p-Smad1 and quantified for positive stained nuclei. Eng+/+ and Eng+/- mice treated with LDN or placebo. Representative images of heart sections 14 days post-MI are shown. N=5-16 mice per group. b   Paraffin heart sections were stained for p-Smad2 staining and quantified for positive stained nuclei. Eng+/+ and Eng+/- mice treated with LDN or placebo. Representative images of heart sections 14 days post-MI are shown. N=5-16 mice per group. Scale bars: 30μm. *p<0.05; #p<0.001

LDN treatment improves cardiac function

Since LDN influences the TGFβ response in *Eng*^{+/-} *in vitro*, we next investigated whether LDN may influence the impaired cardiac recovery of *Eng*^{+/-} mice after MI. LDN was systemically administered 2-14 days after the induction of MI. The efficacy of the LDN treatment was confirmed by a reduction in the number of cells positive for phosphorylated Smad1 (Fig. 5a) and an increased number of cells expressing phosphorylated Smad2 (Fig. 5b) 14 days post-MI. In both WT and *Eng*^{+/-} mice, LDN treatment significantly improved cardiac function (Fig. 6a, p=0.02 and p=0.03 respectively) and reduced infarct size (Fig. 6b, p=0.02 and p<0.001 respectively). Investigating the infarct border zone of these mice in more detail revealed that LDN treatment increased capillary density in WT hearts, but had no effect on the number of capillaries in *Eng*^{+/-} mice. Interestingly, LDN treatment did not change the number of arteries in WT hearts, whereas in *Eng*^{+/-} animals the number of arteries significantly increased (Fig. 6c, quantification in 6d, 6e, p<0.05).

LDN treatment improves perfusion recovery after Hind Limb Ischemia

Eng^{+/-} mice have a delayed perfusion recovery after induction of ischemia in the mouse hind limb (Fig. 7)[4]. Therefore, to determine whether the effect of LDN was specific for the heart or a more general response of endoglin heterozygosity to an ischemic insult, we chose the hind limb ischemia model in addition to the experimentally induced MI. After ligation of the femoral artery, *Eng*^{+/-} or WT mice were treated with LDN or vehicle and perfusion recovery was measured by Laser Doppler Perfusion Imaging (LDPI) at day 7 post ligation. Interestingly, while blood flow in the hind limb of WT mice was not different between LDN or vehicle treated animal, LDN treatment significantly improved the hampered paw perfusion in *Eng*^{+/-} mice (Fig. 7, p=0.002). Overall, we conclude that tissue repair in *Eng*^{+/-} mice after ischemic damage in both experimentally induced myocardial and hind limb ischemia was improved by LDN treatment, suggesting that LDN treatment has a general beneficial effect on ischemic tissue repair.

Discussion

The natural response of the body to ischemic injury is to stimulate neovascularization. The influx of circulating monocytes is important for cardiac repair post MI and contributes to the revascularization of ischemic tissue[35,36]. The pro-angiogenic role of endoglin, a TGFβ co-receptor, in vascular development is well established[26,37,38]. We have previously reported that the enhanced deterioration of cardiac function after experimentally induced MI in *Eng*^{+/-} mice results from impaired capacity of HHT1 MNCs to home to the site of injury and accumulate in the infarct zone to stimulate vessel formation[5,39]. In this study, we show that monocytes are depending on the expression of endoglin to be able to differentiate from an inflammatory M1 macrophage towards a regenerative M2 macrophage and endoglin heterozygosity prolongs the inflammatory response after myocardial infarction. This observation may explain why patients[1,40,41] and mice[3,11] haplo-insufficient for endoglin show prolonged inflammation and delayed wound healing and tissue repair after injury.

We demonstrated that TGFβ differently influenced the differentiation of wild type versus *Eng*^{+/-} or HHT1 macrophages. Wild type monocytes differentiate to M2 macrophages in an ALK5 dependent manner while inhibition of the BMP type I receptors did not influence their differentiation. Macrophages heterozygous for endoglin did not differentiate towards
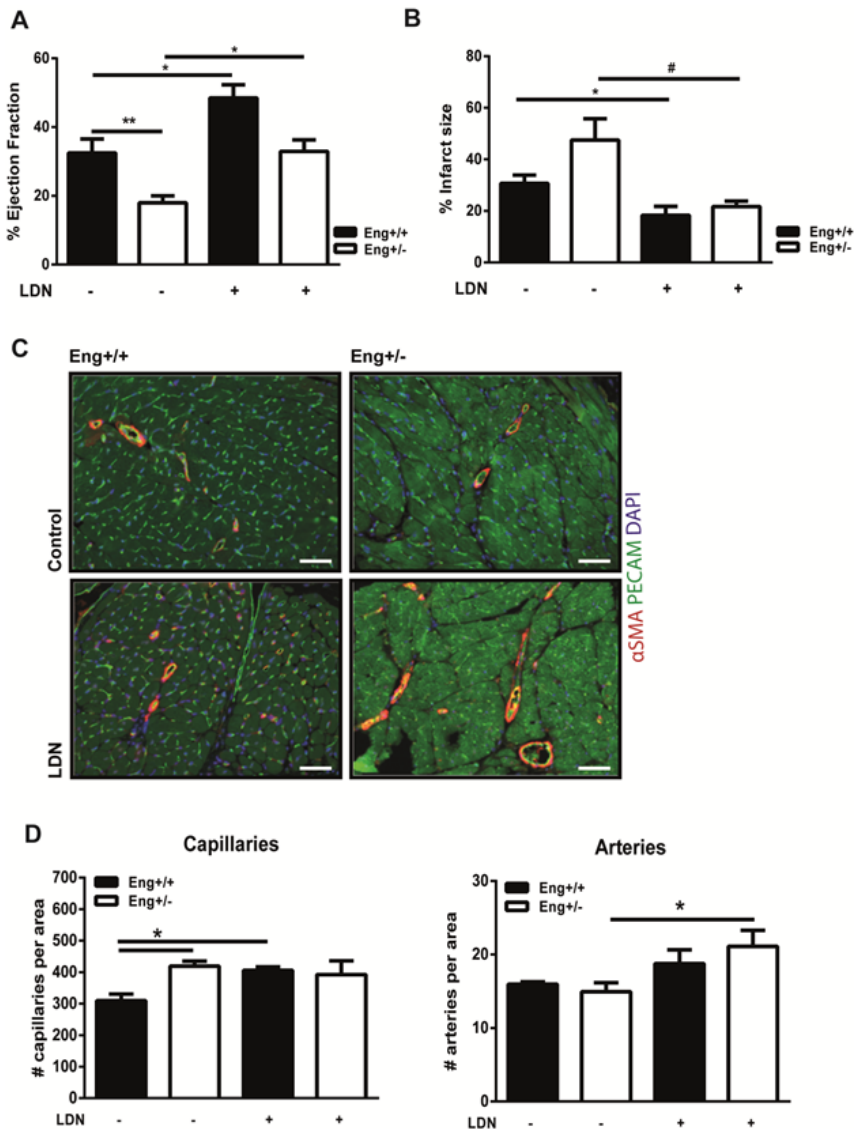
Fig. 6 LDN restores cardiac function in Eng+/- to normal levels 14 days after MI.
a Cardiac ejection fraction percentage of Eng+/+ and Eng+/- mice 14 days post-MI, treated with
LDN or placebo. N=5-16 mice per group. b Infarct size was determined in both Eng+/+ and Eng+/-
mice using Picrosirius Red staining. Top row: representative pictures of murine transversal heart
sections with infarct size (purple) determined by Picrosirius Red staining. 1.0x magnification.
Bottom, quantification of infarcted area as percentage of total LV area. N=5-16 mice per group.
c-d LDN treatment influences cardiac neo-vascularization post-MI. c Paraffin sections of mouse
heart tissue were analyzed for the number of capillaries by staining for PECAM (green) and
arteries by analyzing the expression of αSMA (red) and PECAM (green). N=5-16 mice per group.
d Quantification of the number of capillaries (left) and arteries (right) in Eng+/+ and Eng+/- mice
treated with or without LDN. N=5-16 mice per group. Scale bar: 50µm. * p<0.05; **p<0.01;
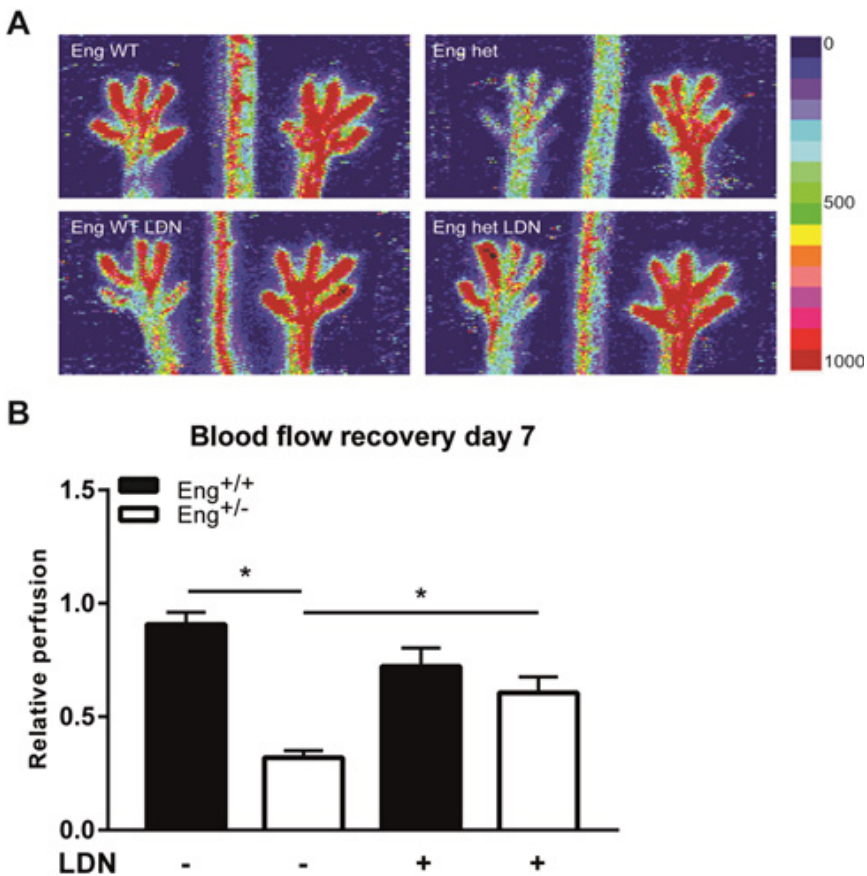**#p<0.001**

Fig. 7 Hind limb blood flow recovery in female mice increases with LDN treatment.
a Representative images of blood flow recovery in the paws as measured by laser Doppler perfusion imaging (LDPI), 7 days after HLI and subsequent treatment with LDN. Colors indicate the level of flow as indicated on the right panel of the figure. The left side limb has HLI, the right side limb was used as control. b Quantification of LDPI measurements, N=5-7 female mice per group. Black bars= WT, white bars= Eng+/-.* p<0.05.

M2 upon TGFβ stimulation, while inhibition of BMP-signaling resulted in a shift towards M2 macrophages. TGFβ is well known as an anti-inflammatory/pro-fibrotic cytokine and is mainly secreted by M2 macrophages[42,43]. We have previously shown that there was no difference in TGFβ, TβRII, ALK1 and ALK5 expression in WT vs HHT1 mononuclear cells[5], and endothelial cells deprived of endoglin expression are unable to process and secrete active TGFβ[44]. We hypothesized that the defect in TGFβ/BMP ligand processing due to deficiency in the co-receptor endoglin could play a role in the impaired TGFβ-directed differentiation of *Eng*^{+/-} macrophages and explain why inhibition of BMP signaling can restore defective endoglin/TGFβ signaling. The absence of endoglin may skew the tight balance that often exists between TGFβ and BMP signaling, and inhibition of the BMP type I receptor kinases may push this balance towards enhanced TGFβ signaling, thereby restoring M2 macrophage differentiation.

The main defect observed in TGFβ signaling in *Eng*^{+/-} monocytes was related to the non-Smad signaling pathway. *Eng*^{+/-} macrophages were still able to signal via the canonical TGFβ/Smad pathway and phosphorylation of Smad2 was significantly increased in combination with LDN treatment. We did observe reduced activation of the non-canonical MAPK/ERK pathway. An overall misbalance in ERK and p38 signaling has a pronounced effect on inflammation status and in reaction to stress[45]. Previous studies have reported the involvement of endoglin in the MAPK/ERK pathway. In dermal fibroblasts, endoglin haploinsufficiency did not affect basal or TGFβ induced pERK1/2 while the basal levels of Akt show a higher degree of phosphorylation[46]. In endothelial cells the activation levels of Akt were not different between WT and *Eng*^{+/-} cells, while ERK and p38 were more active in *Eng*^{+/-} endothelial cells[47]. We show that in macrophages heterozygous for endoglin, ERK1/2 phosphorylation is impaired and neither stimulation nor inhibition of TGFβ signaling resulted in the phosphorylation of ERK1/2. ERK signaling is involved in cell growth and differentiation[48], and may affect apoptosis[49]. Defects in these aforementioned processes could explain the prolonged inflammatory status we observed in *Eng*^{+/-} mice. In addition to impaired ERK activation, *Eng*^{+/-} macrophages showed decreased phosphorylation of p38 in response to TGFβ stimulation and BMP inhibition. P38 is involved in TGFβ-directed monocyte migration and inhibits monocyte proliferation[50], also has anti-angiogenic properties and is reported to be involved in maintaining proper balance in the angiogenic response[51]. Phosphorylated p38 was reported to inhibit VEGF signaling[52], and *Eng*^{+/-} cells exhibit increased VEGF expression[47]. We hypothesize that reduced levels of p-p38 could therefore be involved in the endothelial hyperplasia and impaired angiogenesis found in HHT1 patients[53,54].

In summary, the present data shows that the inability of MNCs from HHT1 patients to induce neoangiogenesis post-MI is not solely due to impaired recruitment of the MNCs to the site of injury[39], but impaired macrophage differentiation, mainly towards an inflammatory phenotype, will also disturb myocardial repair. The impaired differentiation towards the regenerative M2 macrophage subtype due to endoglin heterozygosity could be restored by LDN stimulation, inhibiting BMP type I receptors, confirming both BMP-dependent and non-canonical modulation of macrophage function in HHT1. Furthermore, cardiac ejection fraction after MI and reperfusion recovery after HLI were improved with LDN treatment. Cumulatively, our results imply that treating HHT1 patients with a BMP type I receptor inhibitor would improve tissue repair. Interestingly, more target specific BMP inhibition methods are already being tested in clinical trials as anti-angiogenesis therapy in cancer patients[55]. Overall, inhibition of the BMP signaling pathway can direct regenerative macrophage differentiation and could be considered as a novel therapeutic target in patients with ischemic tissue damage.

Author Contributions
C.D and M.J.G wrote the main manuscript text. C.D, W.B, K.L, M.d.V and K.W performed experiments. C.D, W.B and M.d.V prepared the figures. All authors reviewed the manuscript.

Competing financial interests
The authors declare no competing financial interests.

References

1.   Guilhem, A., Malcus, C., Clarivet, B. & Plauchu, H. Immunological abnormalities associated with hereditary haemorrhagic telangiectasia. 351-362 (2013).

2.   Pérez-Gómez, E.*, et al.* Impaired wound repair in adult endoglin heterozygous mice associated with lower NO bioavailability. *The Journal of investigative dermatology* **134**, 247-255 (2014).

3.   Peter, M.R.*, et al.* Impaired Resolution of Inflammation in the Endoglin Heterozygous Mouse Model of Chronic Colitis. *Mediators of Inflammation* **2014**, 1-13 (2014).

4.   Seghers, L.*, et al.* Shear induced collateral artery growth modulated by endoglin but not by ALK1. *Journal of Cellular and Molecular Medicine* **16**, 2440-2450 (2012).

5.   van Laake, L.W.*, et al.* Endoglin Has a Crucial Role in Blood Cell-Mediated Vascular Repair. *Circulation* **114**, 2288-2297 (2006).

6.   Torsney, E., Charlton, R., Parums, D., Collis, M. & Arthur, H.M. Inducible expression of human endoglin during inflammation and wound healing in vivo. *Inflammation research : official journal of the European Histamine Research Society ... [et al.]* **51**, 464-470 (2002).

7.   Rossi, E.*, et al.* Endothelial endoglin is involved in inflammation: role in leukocyte adhesion and transmigration. *Blood* **121**, 403-415 (2013).

8.   Rossi, E., Lopez-Novoa, J.M. & Bernabeu, C. Endoglin involvement in integrin-mediated cell adhesion as a putative pathogenic mechanism in hereditary hemorrhagic telangiectasia type 1 (HHT1). *Frontiers in genetics* **5**, 457 (2014).

9.   Aristorena, M.*, et al.* Expression of endoglin isoforms in the myeloid lineage and their role during aging and macrophage polarization. *Journal of cell science* **127**, 2723-2735 (2014).

10.   Sanz-Rodriguez, F.*, et al.* Mutation analysis in Spanish patients with hereditary hemorrhagic telangiectasia: deficient endoglin up-regulation in activated monocytes. *Clinical chemistry* **50**, 2003-2011 (2004).

11.   Ojeda-Fernández, L.*, et al.* Mice Lacking Endoglin in Macrophages Show an Impaired Immune Response. *PLOS Genetics* **12**, e1005935 (2016).

12.   Zhang, R.*, et al.* Persistent infiltration and pro-inflammatory differentiation of monocytes cause unresolved inflammation in brain arteriovenous malformation. *Angiogenesis* **19**, 1-11 (2016).

13.   Goumans, M.J. & Ten Dijke, P. TGF-beta Signaling in Control of Cardiovascular Function. *Cold Spring Harb Perspect Biol* (2017).

4

14.	Goumans, M.J., Zwijsen, A., Ten Dijke, P. & Bailly, S. Bone Morphogenetic Proteins in Vascular Homeostasis and Disease. *Cold Spring Harb Perspect Biol* (2017).

15.	Doetschman, T*., et al.* Transforming growth factor beta signaling in adult cardiovascular diseases and repair. *Cell and tissue research* **347**, 203-223 (2012).

16.	Ishida, Y., Kondo, T., Takayasu, T., Iwakura, Y. & Mukaida, N. The Essential Involvement of Cross-Talk between IFN-gamma and TGF-beta in the Skin Wound-Healing Process. *The Journal of Immunology* **172**, 1848-1855 (2004).

17.	Kulkarni, A.B*., et al.* Transforming growth factor beta 1 null mutation in mice causes excessive inflammatory response and early death. *Proceedings of the National Academy of Sciences of the United States of America* **90**, 770-774 (1993).

18.	Larsson, J. Abnormal angiogenesis but intact hematopoietic potential in TGF-beta type I receptor-deficient mice. *The EMBO Journal* **20**, 1663-1673 (2001).

19.	Russell, N.S*., et al.* Blood and lymphatic microvessel damage in irradiated human skin: The role of TGF-β, endoglin and macrophages. *Radiotherapy and Oncology* **116**, 455-461 (2015).

20.	Shull, M.M*., et al.* Targeted disruption of the mouse transforming growth factor-β1 gene results in multifocal inflammatory disease. *Nature* **359**, 693-699 (1992).

21.	Grainger, D.J., Mosedale, D.E. & Metcalfe, J.C. TGF-β in blood: a complex problem. *Cytokine & Growth Factor Reviews* **11**, 133-145 (2000).

22.	Wan, M*., et al.* Injury-activated transforming growth factor β controls mobilization of mesenchymal stem cells for tissue remodeling. *Stem cells* **30**, 2498-2511 (2012).

23.	Chuva de Sousa Lopes, S.M*., et al.* Connective tissue growth factor expression and Smad signaling during mouse heart development and myocardial infarction. *Dev Dyn* **231**, 542-550 (2004).

24.	Goumans, M.-j., van Zonneveld, A.J. & ten Dijke, P. Transforming Growth Factor β–Induced Endothelial-to-Mesenchymal Transition: A Switch to Cardiac Fibrosis? *Trends in Cardiovascular Medicine* **18**, 293-298 (2008).

25.	Goumans, M.J., Liu, Z. & Ten Dijke, P. TGF-beta signaling in vascular biology and dysfunction. *Cell research* **19**, 116-127 (2008).

26.	Lebrin, F*., et al.* Endoglin promotes endothelial cell proliferation and TGF-β/ALK1 signal transduction. *The EMBO journal* **23**, 4018-4028 (2004).

27.	Nahrendorf, M*., et al.* The healing myocardium sequentially mobilizes two monocyte subsets with divergent and complementary functions. *The Journal of experimental medicine* **204**, 3037-3047 (2007).

28.	Mills, C.D., Harris, R.A. & Ley, K. Macrophage Polarization: Decisions That Affect Health. *Journal of clinical & cellular immunology* **6**(2015).

29.	Dingenouts, C.K.E*., et al.* Inhibiting DPP4 in a mouse model of HHT1 results in a shift towards regenerative macrophages and reduces fibrosis after myocardial infarction. *PLoS One* **12**, e0189805 (2017).

30.	Welten, S.M.J*., et al.* Inhibition of 14q32 MicroRNAs miR-329, miR-487b, miR-494, and miR-495 increases neovascularization and blood flow recovery after ischemia. *Circulation Research* **115**, 696-708 (2014).

31.   Duim, S.N., Kurakula, K., Goumans, M.J. & Kruithof, B.P.T. Cardiac endothelial cells express Wilms' tumor-1. Wt1 expression in the developing, adult and infarcted heart. *Journal of Molecular and Cellular Cardiology* **81**, 127-135 (2015).

32.   Massagué, J. How cells read TGF-beta signals. *Nature reviews. Molecular cell biology* **1**, 169-178 (2000).

33.   Nakagawa, T.*, et al.* Role of ERK1/2 and p38 mitogen-activated protein kinases in the regulation of thrombospondin-1 by TGF-beta1 in rat proximal tubular cells and mouse fibroblasts. *Journal of the American Society of Nephrology : JASN* **16**, 899-904 (2005).

34.   Zhang, Y.E. Non-Smad Signaling Pathways of the TGF-beta Family. *Cold Spring Harb Perspect Biol* **9**(2017).

35.   Frangogiannis, N.G. The inflammatory response in myocardial injury, repair, and remodelling. *Nature Reviews Cardiology* **11**, 255-265 (2014).

36.   Gombozhapova, A.*, et al.* Macrophage activation and polarization in post-infarction cardiac remodeling. *J Biomed Sci* **24**, 13 (2017).

37.   ten Dijke, P., Goumans, M.-J. & Pardali, E. Endoglin in angiogenesis and vascular diseases. *Angiogenesis* **11**, 79-89 (2008).

38.   Tual-Chalot, S.*, et al.* Endothelial depletion of Acvrl1 in mice leads to arteriovenous malformations associated with reduced endoglin expression. *PloS one* **9**(2014).

39.   Post, S.*, et al.* Impaired recruitment of HHT-1 mononuclear cells to the ischaemic heart is due to an altered CXCR4/CD26 balance. *Cardiovascular Research* **85**, 494-502 (2010).

40.   Dupuis-Girod, S.*, et al.* Hemorrhagic hereditary telangiectasia (Rendu-Osler disease) and infectious diseases: an underestimated association. *Clinical infectious diseases: an official publication of the Infectious Diseases Society of America* **44**, 841-845 (2007).

41.   Mathis, S.*, et al.* Cerebral abscesses in hereditary haemorrhagic telangiectasia: a clinical and microbiological evaluation. *Clinical neurology and neurosurgery* **114**, 235-240 (2012).

42.   Braga, T.T., Agudelo, J.S.H. & Camara, N.O.S. Macrophages during the fibrotic process: M2 as friend and foe. *Frontiers in Immunology* **6**, 1-8 (2015).

43.   Vernon, M.A. & Mylonas, K.J. Macrophages and Renal Fibrosis. *Seminars in Nephrology* **30**, 302-317 (2010).

44.   Carvalho, R.L.*, et al.* Defective paracrine signalling by TGFbeta in yolk sac vasculature of endoglin mutant mice: a paradigm for hereditary haemorrhagic telangiectasia. *Development* **131**, 6237-6247 (2004).

45.   Kebir, D.E. & Filep, J.G. Modulation of neutrophil apoptosis and the resolution of inflammation through β2 integrins. *Frontiers in Immunology* **4**, 1-15 (2013).

46.   Pericacho, M.*, et al.* Endoglin Haploinsufficiency Promotes Fibroblast Accumulation during Wound Healing through Akt Activation. *PLoS ONE* **8**, e54687 (2013).

47.   Park, S.*, et al.* Endoglin regulates the activation and quiescence of endothelium by participating in canonical and non-canonical TGF- signaling pathways. *Journal of Cell Science* **126**, 1392-1405 (2013).

4

48.		Monick, M.M.*, et al.* Constitutive ERK MAPK activity regulates macrophage ATP production and mitochondrial integrity. *Journal of immunology (Baltimore, Md. : 1950)* **180**, 7485-7496 (2008).

49.		Sawatzky, D.A., Willoughby, D.A., Colville-Nash, P.R. & Rossi, A.G. The Involvement of the Apoptosis-Modulating Proteins ERK 1/2, Bcl-xL and Bax in the Resolution of Acute Inflammation in Vivo. *The American Journal of Pathology* **168**, 33-41 (2006).

50.		Olieslagers, S., Pardali, E., Tchaikovski, V., Ten Dijke, P. & Waltenberger, J. TGF-β1/ALK5-induced monocyte migration involves PI3K and p38 pathways and is not negatively affected by diabetes mellitus. *Cardiovascular Research* **91**, 510-518 (2011).

51.		Aguirre-Ghiso, J.A. Models, mechanisms and clinical evidence for cancer dormancy. *Nature Reviews Cancer* **7**, 834-846 (2007).

52.		Gomes, E. & Rockwell, P. p38 MAPK as a negative regulator of VEGF/VEGFR2 signaling pathway in serum deprived human SK-N-SH neuroblastoma cells. *Neurosci Lett* **431**, 95-100 (2008).

53.		Abdalla, S.A. Hereditary haemorrhagic telangiectasia: current views on genetics and mechanisms of disease. *Journal of Medical Genetics* **43**, 97-110 (2005).

54.		Thalgott, J., Dos-Santos-Luis, D. & Lebrin, F. Pericytes as targets in hereditary hemorrhagic telangiectasia. *Frontiers in Genetics* **5**, 1-16 (2015).

55.		de Vinuesa, A.G., Bocci, M., Pietras, K. & ten Dijke, P. Targeting tumour vasculature by inhibiting activin receptor-like kinase (ALK)1 function. *Biochemical Society Transactions* **44**, 1142-1149 (2016).

4